MDPI

Article

Disturbances of Doppler Frequency Shift of Ionospheric Signal and of Telluric Current Caused by Atmospheric Waves from Explosive Eruption of Hunga Tonga Volcano on January 15, 2022

Nazyf Salikhov [1,2], Alexander Shepetov [1,2,*], Galina Pak [1], Vladimir Saveliev [1,3], Serik Nurakynov [1], Vladimir Ryabov [2] and Valery Zhukov [2]

1   Institute of Ionosphere, Almaty 050020, Kazakhstan
2   P. N. Lebedev Physical Institute of the Russian Academy of Sciences, 119991 Moscow, Russia
3   V. G. Fesenkov Astrophysical Institute, Almaty 050020, Kazakhstan
*   Correspondence: ashep@tien-shan.org

Abstract: After the explosive eruption of the Hunga Tonga volcano on 15 January 2022, disturbances were observed at a distance of about 12,000 km in Northern Tien Shan and regarded variations in the atmospheric pressure, in telluric current, and in the Doppler frequency shift of ionospheric signal. At 16:00:55 UTC, a pulse of atmospheric pressure was detected there, with peak amplitude of 1.3 hPa and propagation speed of 0.3056 km/s, equal to the velocity of Lamb waves. In the variations in the Doppler frequency shift, disturbances of two types were registered on the 3212 km and 2969 km long inclined radio paths, one of which arose as a response to the passage of a Lamb wave (0.3059 km/s) through the reflection point of the radio wave and another as reaction to an acoustic-gravity wave (0.2602 km/s). Two successive perturbations were also detected in the records of telluric current at the arrival times of the Lamb and acoustic-gravity waves at the registration point. According to the parameters of the Lamb wave, the energy transfer into the atmosphere upon the explosion of the Hunga Tonga volcano was roughly estimated to be 2000 Mt of TNT equivalent.

Keywords: Hunga Tonga volcano eruption; Doppler frequency shift; ionosphere; telluric current; atmospheric pressure; Lamb wave; acoustic-gravity wave

1. Introduction

The explosive eruption of the Hunga Tonga–Hunga Ha´apai volcano in the South West Pacific, which happened on 15 January 2022, was the first event of the current century with a volcanic explosivity index of 5. Unique to this event are the powerful disturbances that were observed across the entire thickness of the atmosphere. Everywhere around the globe, the appearance of intensive infrasonic, acoustic-gravity, and Lamb waves was detected. On-ground barometers in different parts of the world registered the atmospheric signatures of the volcano explosion [1–3], and the atmospheric Lamb wave bypassed the Earth several times, propagating at the mean velocity of ∼0.3 km·s^{-1} [4–6]. Disturbances of the ionosphere caused by the Hunga Tonga explosive eruption were studied by means of the Global Navigation Satellite System (GNSS) receiver net, which is commonly used for measuring the total electron concentration in the ionosphere [3,6–8]. Together with the ground-based GNSS measurements, the prominent ionospheric effects induced by the Hunga Tonga volcano explosion were also observed by the satellites of the ICE and GOLD missions, situated, correspondingly, in the low Earth and geostationary orbits [9].

Generally, it is known that large volcano eruptions cause ionospheric disturbances of various kinds [10,11], which are believed to arise from the upward leakage of the energy of Lamb waves. Energy can be transmitted into the ionosphere through atmospheric resonance

at the frequency of acoustic-gravity oscillations, which stipulates the large amplitude of the waves at high altitudes [8]. In the case of the Hunga Tonga event, the GNSS receivers identified two types of traveling ionospheric disturbances (TIDs) that propagated from the epicenter of the explosion: there were two large-scale and several medium-scale TIDs. The most dominant medium-scale TID moved at a velocity of about $(200–400)\,\mathrm{m\cdot s^{-1}}$ and coincided with the disturbance of the near-surface atmospheric pressure [7]. In a multi-sensor study of the propagation of ionospheric disturbances from the Hunga Tonga volcano explosion, which was based on more than 5000 GNSS receivers distributed around the whole globe, it was demonstrated that the ionosphere is a sensitive detector of atmospheric waves and geophysical perturbations [8].

In recent decades, continuous multi-parametric observations of the geophysical environment have been performed in Northern Tien Shan, at radio polygon "Orbita" of Institute of Ionosphere and at the Tien Shan mountain scientific station of P. N. Lebedev Physical Institute [12,13]. The experimental base is situated in a mountainous, seismically active locality and encompasses complex measuring equipment for the simultaneous investigation of the processes that take place in the lithosphere, atmosphere, and ionosphere. The eruption of the Hunga Tonga volcano was one of the most powerful explosive volcanic events of the modern era, the disturbances of which were distributed from the lithosphere to the heights of the ionosphere and even spread into near space. This event represents a unique natural experiment with strong impact on the environment, which was the motif to search for its geophysical consequences using the detectors of the Tien Shan scientific complex.

In the present study, the response of the ionosphere to the Hunga Tonga explosive eruption event was investigated at the distances of $(11–12)\cdot 10^3\,\mathrm{km}$ from the volcano using the method of the continuous variation monitoring of the Doppler frequency shift of the ionospheric signal on inclined radio paths [14,15]. The method of Doppler sounding, primarily applied in this work, has demonstrated its efficiency and high sensitivity in a number of studies of the ionospheric disturbances that accompany powerful explosions, earthquakes, solar flares, and geomagnetic storms [16–21]. Together with the Doppler signal, the most convincing effects of the Hunga Tonga volcanic explosion were found among the measurements of the atmospheric pressure and telluric current, whose data are also discussed in this article.

2. Experimental Technique

The investigation of the response of geophysical fields to the Hunga Tonga–Hunga Ha´apai volcano eruption was carried out at two high-altitude experimental sites: radio polygon "Orbita" of Institute of Ionosphere (N43.05831, E76.97361; 2750 m above the sea level) and the Tien Shan mountain scientific station of Lebedev Physical Institute (N43.03519, E76.94139; 3340 m a.s.l.). Both sites are located in the territory of the Republic of Kazakhstan in Tien Shan mountains, 2.9 km apart from each other, at a distance of 12,948 km from the Hunga Tonga volcano island.

2.1. Barometric Pressure

Continuous monitoring of the atmospheric pressure is performed at the Tien Shan mountain station using a MSB181-type digital barometer (LLC "MicroStep-MIS", Russia), which permits researchers to measure the pressure in the range of $(600–1100)\,\mathrm{hPa}$ with precision of $\pm 0.3\,\mathrm{hPa}$. The barometric data with one-minute time resolution are accessible in real time on an Internet site of the Tien Shan mountain station [22].

2.2. Doppler Frequency Shift of Ionospheric Signal on Inclined Radio Paths

For the detection of the ionospheric response to the volcano eruption, we used a combined hard- and software technique of Doppler measurements that is based on the phase-locked loop (PLL) principle and permits one to measure the Doppler shift of a larger-amplitude radio signal under the conditions of multi-path signal propagation [14]. Within a 15 Hz wide hold-off band of the PLL loop, the non-linearity of the frequency conversion

characteristic equaled 0.46%, which is quite sufficient for the high-quality estimation of the Doppler shift of a radio signal reflected from the ionosphere. The frequency of the radio receiving part of the hardware used was stabilized with a rubidium frequency standard, such that the precision of Doppler shift measurement, 0.01 Hz or better, was 1.5–2 orders below the level of the background frequency variation in the F-region of the ionosphere. The receiving part of the instrument was placed at radio polygon "Orbita", and as a source of sounding signal, the transmitters of broadcasting radio stations were used. The selection of optimal transmitter frequencies for the day- and nighttime was made accordingly to Short-Wave Radio Frequencies BBC Catalog [23]; frequency switching during the measurements was made automatically with a special computer program, taking into account the time of day and the yearly season. The highly automated operation mode of the whole Doppler ionosonde equipment makes it possible to perform continuous, all-day registration of the Doppler frequency shift of ionospheric signals.

In the present experiment, the monitoring of the Doppler frequency shift was made on two inclined radio paths, Beijing radio polygon "Orbita" (length of $d = 3200$ km and basic frequency of $f = 7275$ kHz) and Kuwait radio polygon "Orbita" ($d = 3950$ km and $f = 5860$ kHz). The left graph in Figure 1 illustrates the mutual disposition of both mentioned radio paths and of the Hunga Tonga volcano. The distance from the volcano to the projection on the Earth of the point of radio wave reflection equaled 11,393 km for the radio path Beijing radio polygon "Orbita" and to 14,367 km for the Kuwait radio polygon "Orbita" path. Both distances were estimated using the Garmin MapSource program.
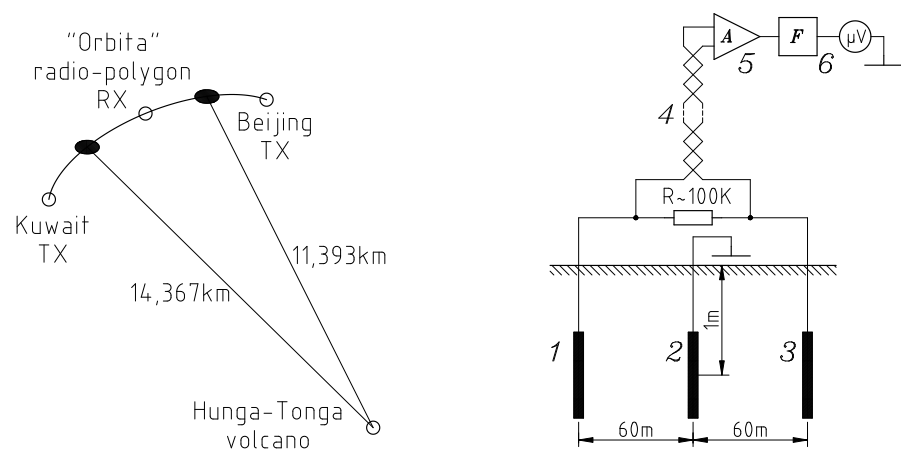
Figure 1. Left: Disposition scheme of radio paths used in the Doppler sounding experiment relative to the Hunga Tonga volcano: radio transmitters *(TX)* and receiver *(RX)* at radio polygon "Orbita". Two hatched ellipses indicate the projection of the radio wave reflection points onto the Earth. Right: Scheme of equipment for measurement of telluric current at the Tien Shan mountain station: *(1),(2),(3)* three buried electrodes, *(4)* a ~20 m long pair of twisted wires, *(5)* a differential amplifier, and *(6)* an active filtering scheme.

2.3. Measurements of Telluric Current

The point of telluric current measurement is situated at the Tien Shan mountain station, in a locality far away from any industrial sources of electromagnetic interference [24]. The measuring equipment consisted of three lead electrodes of rectangular shape, $410 \times 80 \times 10$ mm^3, buried in vertical position at a depth of 1 m below the surface of the ground, such that the distance between the two outer electrodes equals 120 m. As it is shown in the right plot of Figure 1, the signal of the current was gathered from the two side electrodes, while the middle one was used as the zero point of the electric measurement scheme. For the suppression of in-phase interference, the signal from the electrodes was connected to the measurement equipment through a twisted pair of wires and a differential

amplifier. The registration of the weak electric oscillations induced on the electrodes by telluric current proceeded in the range of extremely low frequencies, (0–20) Hz.

For the selection of weak electric signals with typical amplitude of a few tens–hundred of microvolts, it is necessary to eliminate the main stray of industrial power from the useful signal of telluric current. In the considered experiment, a notch filter was applied for the ~40 dB rejection of the industrial 50 Hz interference. The main filtration of the input signal was made by a 12-order Chebyshev low-pass filter with cutoff frequency of 32 Hz and ⩾80 dB suppression of high-frequency oscillations above the cutoff. The active filtering scheme was built on the basis of precision low-noise operational amplifiers OPA-27GP of Texas Instruments production. The final registration of the purified signal was made by a 12-bit ADC continuously operating at the digitization speed of 80 sps [24].

3. Results and Discussion

3.1. Anomaly of Atmospheric Pressure

On 15 January 2022, on the day of the Hunga Tonga volcano explosive eruption, the barometer located in the territory of the Tien Shan mountain station registered a short-time anomalous pulse of the atmospheric pressure, as illustrated in Figure 2. As it follows from this plot, the peak amplitude of pressure growth above the preceding level of undisturbed slow variation was about (1.3–1.4) hPa, and the whole effect lasted about (25–30) min. The start of the atmospheric pressure pulse was detected at the moment of 16:00:55 UTC, nearly 12 h after the Hunga Tonga volcano explosion.
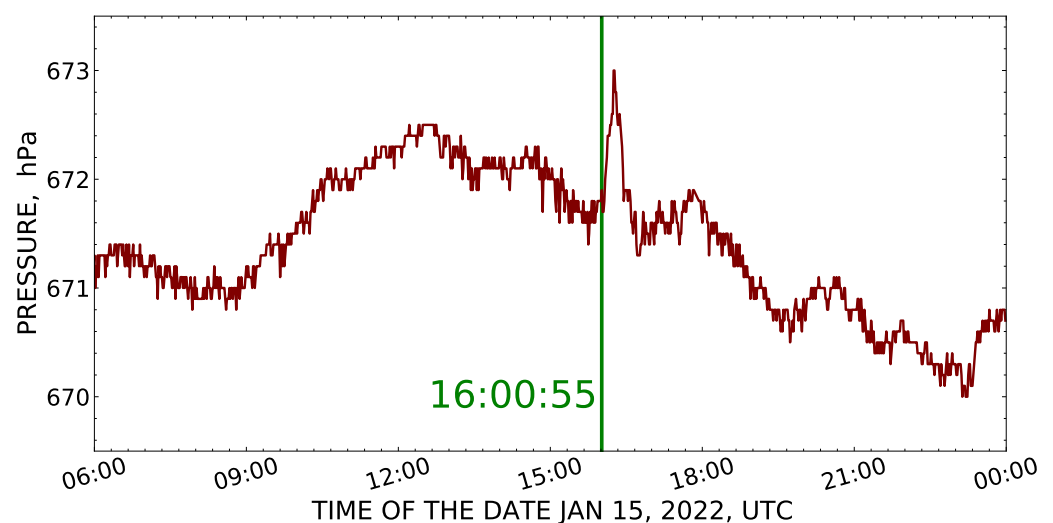
Figure 2. Pulse of atmospheric pressure registered at the Tien Shan mountain station on 15 January 2022.

Similarly, anomalous short-time pulses of the atmospheric pressure were detected on the same day of the Hunga Tonga volcanic event by barometric equipment installed in various points of the globe. A number of the atmospheric pressure time series registered at that time, including the record of the Tien Shan station, are presented in the upper panel of Figure 3. Except for the Tien Shan station data, the information for these plots was obtained from an open access database [25]. It can be seen that, everywhere, the detected pulses of the atmospheric pressure had similar shape and duration, which varied only slightly among the observation points.
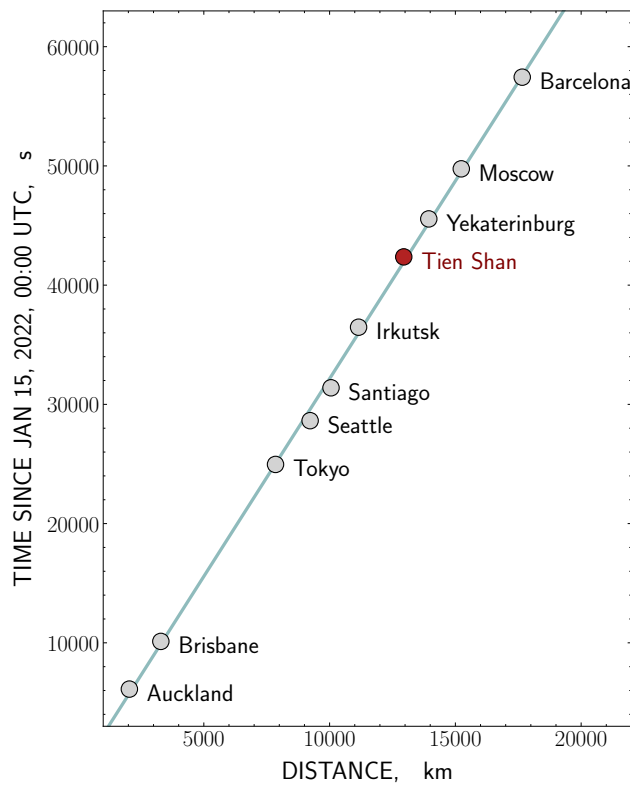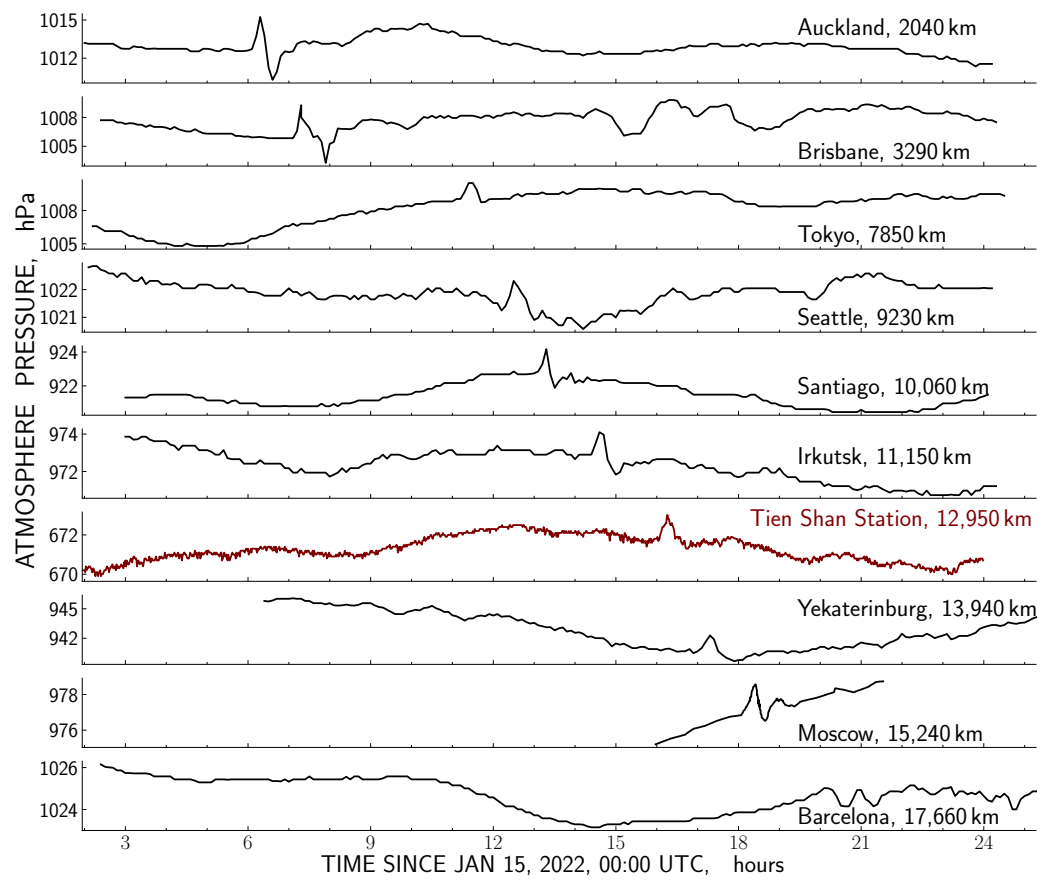
Figure 3. Top: Anomalous pulses of atmospheric pressure detected at various distances from the Hunga Tonga volcano on 15 January 2022. Bottom: Dependence of observation time of atmospheric pressure pulse on distance from the volcano.

In the bottom panel of Figure 3, the moments of the atmospheric pressure pulses are plotted in dependence on the distance between the observation point and the Hunga Tonga volcano. The distances in the bottom plot were defined on the basis of the geographical coordinates of corresponding points with the Garmin MapSource program. Taking into account these distances and the time delays of the pressure pulses, the average propagation velocity of the atmospheric disturbance was calculated, and the values are listed in Table 1.

Table 1. Propagation of pulse of atmospheric pressure detected on 15 January 2022 at various distances from the Hunga Tonga volcano.

Observation Point	Geographical Coordinates	Distance, km	Arrival of Pressure Pulse, UTC	Propagation Time, s	Propagation Speed, km·s^{-1}
Auckland	S36.83970 E174.82843	2040	05:56:44	6119	0.3334
Brisbane	S27.46778 E153.02806	3291	07:03:24	10,119	0.3252
Tokyo	N36.23000 E140.18000	7850	11:10:47	24,962	0.3145
Seattle	N47.64236 W122.33348	9226	12:11:57	28,632	0.3222
Santiago	S33.31831 W70.68514	10,056	12:57:55	31,390	0.3241
Irkutsk	N52.27000 E104.45000	11,152	14:22:37	36,472	0.3058
Tien Shan Station	**N43.04361 E76.94139**	**12,948**	**16:00:55**	**42,370**	**0.3056**
Yekaterinburg	N56.85400 E60.64400	13,943	16:54:00	45,555	0.3061
Moscow	N55.76660 E37.57324	15,235	18:04:09	49,755	0.3061
Barcelona	N41.65060 E2.44564	17,658	20:12:08	57,443	0.3074

As it follows from the data presented in Figure 3 and Table 1, the maximum velocity was observed at the nearest registration points, i.e., in Auckland and Brisbane, and only starting from distances above $\sim 10^4$ km, the atmospheric pressure pulse propagated in the SE–NW direction at a practically constant speed of 0.306 km·s^{-1}.

Positive anomalies of the atmospheric pressure that moved at the velocity of ~ 0.3 km·s^{-1} from SE to NW over the territory of Japan and lasted about 20 min in total were also reported in [6]. According to [26], generally, such pulses of atmospheric pressure are brought by a Lamb wave that propagates at the speed of sound (~ 0.3 km·s^{-1}) along the surface of the Earth.

It should be noted that Barcelona is only situated at a ~ 2100 km distance from the antipode point relative to the Hunga Tonga volcano. This may be the reason why the atmospheric pressure pulse plotted for this station in Figure 3 has a maximally complicated shape with two peaks and double duration; these features can be explained by successive registration of the direct and antipodal Lamb waves moving from the volcano explosion point.

The moment of the atmospheric pressure peak observation at the Tien Shan station, 16:00:55 UTC, agrees well with the general trend of the world data and corresponds to the propagation speed of a surface Lamb wave from the Hunga Tonga volcano explosion. This

agreement permits us to identify the observed anomaly of atmospheric pressure as an effect also connected with the Hunga Tonga volcanic event.

3.2. Doppler Frequency Shift of Ionospheric Signal

The Doppler frequency shift of the ionospheric signal at radio polygon "Orbita" was registered on the two radio paths, Beijing radio polygon "Orbita" and Kuwait radio polygon "Orbita". The optimal radio frequencies for the day- and nighttime were chosen in accordance with Short-Wave Radio Frequencies BBC Catalog [23]. The geometric disposition of both paths relative to the location of the Hunga Tonga volcano is illustrated by a chart in Figure 1.

The continuous monitoring of Doppler frequency on the day of the Hunga Tonga volcano explosion, 15 January 2022, made it possible to reveal two disturbances of the ionosphere, which are illustrated in the plots in Figure 4.
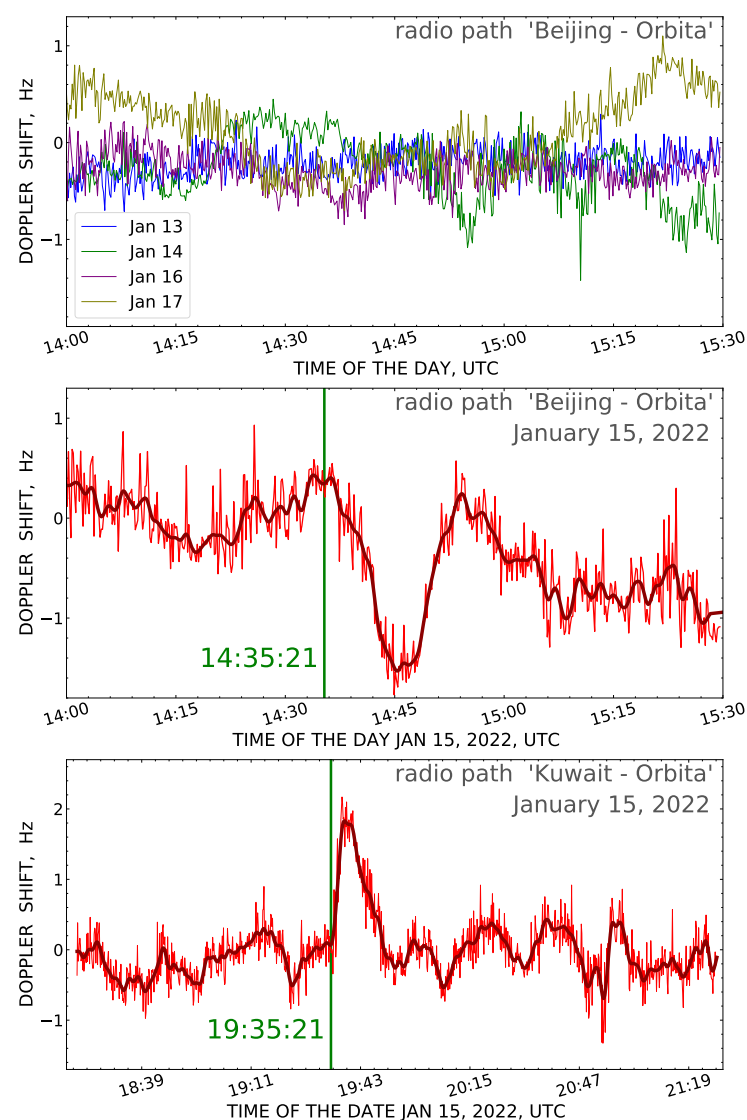
Figure 4. Upper panel: Sample time series of Doppler frequency shift of ionospheric signal registered on radio path Beijing radio polygon "Orbita" on the days of 13, 14, 16, and 17 January 2022. **Middle and bottom panels**: Doppler shift data measured on the paths Beijing radio polygon "Orbita" and Kuwait radio polygon "Orbita" on 15 January 2022. Thin lines correspond to the original measurement data of the Doppler frequency; bold lines, to the same data after their smoothing with a 10-point running average filter.

The upper plot of Figure 4 demonstrates a set of superimposed time series of the Doppler frequency shift of the ionospheric signal that were obtained at the radio path Beijing radio polygon "Orbita" on the dates of 13, 14, 16, and 17 January, i.e., both immediately on the eve of and a few days after the considered volcanic event. It can be seen in this plot that the undisturbed daily records of Doppler data do not differ considerably among the days and generally overlap within the limits of ± 1 Hz.

In contrast to the regular background oscillations observed on the preceding days, on 15 January 2022, a considerable negative disturbance of Doppler frequency at amplitude of about 2 Hz and with duration of 1073 s was detected and is shown in the middle plot of Figure 4. This disturbance appeared at the time of 14:35:21 UTC, i.e., 37,236 s (10.3 h) after the explosion of the Hunga Tonga volcano. Taking into account the distance between the volcano and the reflection point of radio waves on the Beijing radio polygon "Orbita" radio path, 11,393 km, the propagation velocity of the atmospheric disturbance of the ionosphere could be calculated to be 0.3059 km·s^{-1}. As it is discussed above, practically the same value, 0.3056 km·s^{-1}, was obtained at the Tien Shan mountain station for the speed of the pulse of atmospheric pressure that corresponded to the propagation of the Lamb wave from the volcano explosion (see Table 1).

The observed time correlation is evidence that the Lamb wave propagating across the whole thickness of the atmosphere also initiated disturbances of the ionosphere, which revealed themselves in the record of the Doppler frequency shift. As an additional argument in favor of this conclusion, the ICON-MIGHTI and Swarm satellite observations [27] can be mentioned; they recorded the penetration of Lamb waves at the heights of (90–300) km into the ionosphere.

The second anomaly in the Doppler frequency shift of the ionospheric signal found on 15 January 2022 was registered at the time of 19:35:21 UTC, i.e., 55,241 s (15.3 h) after the Hunga Tonga volcano explosion, when the Doppler sounding equipment had just switched into operation on the Kuwait radio polygon "Orbita" radio path. The corresponding time series of Doppler data is presented in the bottom plot of Figure 4. It can be seen that there was a disturbance with a maximum frequency shift of 1.84 Hz and 1270 s duration, followed by a sequence of undulating perturbations at much lesser amplitudes and the quasi-periods of 1223 s, 1146 s, and 1053 s. As it is known, a similar periodicity of 1000 s order can be observed in the propagation of acoustic-gravity waves in the ionosphere [28].

Supposing that the reason of the ionospheric effect detected at 19:35:21 UTC is also connected with the Hunga Tonga volcano explosion and taking into account the 14,367 km distance from the volcano to the radio waves reflection point on the radio path used, a calculation analogous to the above gives the distribution speed of the disturbance as 0.2602 km·s^{-1}. This estimate corresponds well to the velocity of acoustic-gravity waves [5].

The characteristics of the two anomalous effects found during the day of 15 January 2022 in the records of the Doppler frequency shift of the ionospheric signal are summed up in Table 2.

Table 2. Parameters of the ionospheric disturbance propagation on the radio paths Beijing radio polygon "Orbita" and Kuwait radio polygon "Orbita".

Radio Path	Geographical Coordinates of the Radio Wave Reflection Point	Distance from the Reflection Point, km	Time Moment of the Ionospheric Anomaly, UTC	Propagation Time, s	Propagation Speed, km·s^{-1}
Beijing "Orbita"	N43.66260 E96.75869	11,393	14:35:21	37,236	0.3059
Kuwait "Orbita"	N36.89300 E60.39300	14,367	19:35:21	55,241	0.2602

Thus, the data obtained at radio polygon "Orbita" permit us to connect the revealed ionosphere disturbances with the successive propagation of the Lamb and acoustic-gravity waves generated by the explosion of the Hunga Tonga volcano. At the same time, the detected effects demonstrate the effectiveness of the applied method of Doppler sounding on inclined radio paths for revealing ionospheric disturbances of volcanic origin at a distance of more than 10^4 km.

3.3. Measurements of Telluric Current

As it follows from the previous section, powerful atmospheric disturbances, distributed after the explosion of the Hunga Tonga volcano as Lamb waves across the entire atmosphere thickness, also initiated perturbations in the ionosphere. The resulting modulation of the electric currents in the ionosphere caused geomagnetic effects that may have been registered at the ground level as variations in telluric current. This consideration was the reason for searching for anomalies in the monitoring data of telluric current after the Hunga Tonga explosion event.

In Figure 5, the time series of the atmospheric pressure and of the intensity of telluric current recorded at the Tien Shan station on 15 January 2022 are matched.
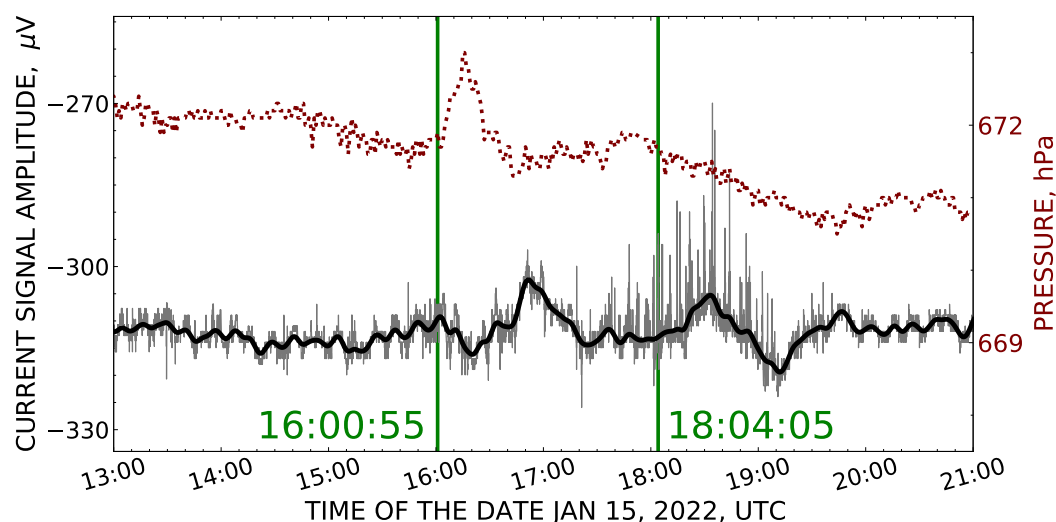
Figure 5. Disturbances of atmospheric pressure and telluric current detected at the Tien Shan station at the passage of acoustic waves from the Hunga Tonga volcano explosion. The dotted line above represents the atmospheric pressure. The thin line in the lower distribution corresponds to the original measurement data of telluric current, while the bold one corresponds to the same data smoothed using a running average filter with a 10-point-long kernel.

As it follows from this figure, at the moment of 16:00:55 UTC, an appreciable (6–10) μV decrease appeared in the record of telluric current, almost simultaneously with the arrival of the atmospheric pressure pulse, which propagated at the speed of 0.3056 km·s^{-1} from the Hunga Tonga volcano point. After the bay-like dip feature in the record, an increase in the telluric current amplitude was observed.

It is worth noting that the decrease in the current lasted about 1800 s, which is comparable to the length of the barometric pressure pulse. The total duration of the whole period of telluric current variations, both of the negative dip and of the subsequent rise, was ~4900 s.

Another noticeable disturbance of the record of telluric current started at 18:04:05 UTC, as it can also be seen in Figure 5. This moment corresponds to the arrival time of the acoustic-gravity wave from the Hunga Tonga volcano, which moved at the speed of 0.260 km·s^{-1} (see Table 2). The second period of the telluric current disturbances lasted about 6800 s.

The described time correlations may be a reason to suppose an electromagnetic nature of the detected disturbances, and the modulation of the electric currents in the ionosphere

by atmospheric waves may result in the variation in the telluric current measured at the ground level.

3.4. Evaluation of Energy Released into the Atmosphere upon Hunga Tonga Volcano Explosion

In Figure 6, the above-considered time history of the Doppler frequency shift of the ionospheric signal on the Beijing radio polygon "Orbita" radio path is superimposed with the record of the atmospheric pressure taken on the date of the Hunga Tonga explosion at the Tien Shan mountain station. The barometric data series in this plot is shifted along the horizontal axis to the time of -1.50 h, in correspondence with the propagation speed of the Lamb acoustic wave from the Hunga Tonga explosion, 0.3056 km·s^{-1} (see Table 1), and the distance difference of 1560 km between the Hunga Tonga volcano and the Tien Shan station, one side, and between the volcano and the reflection point of radio waves on the Beijing radio polygon "Orbita" radio path, on the other.
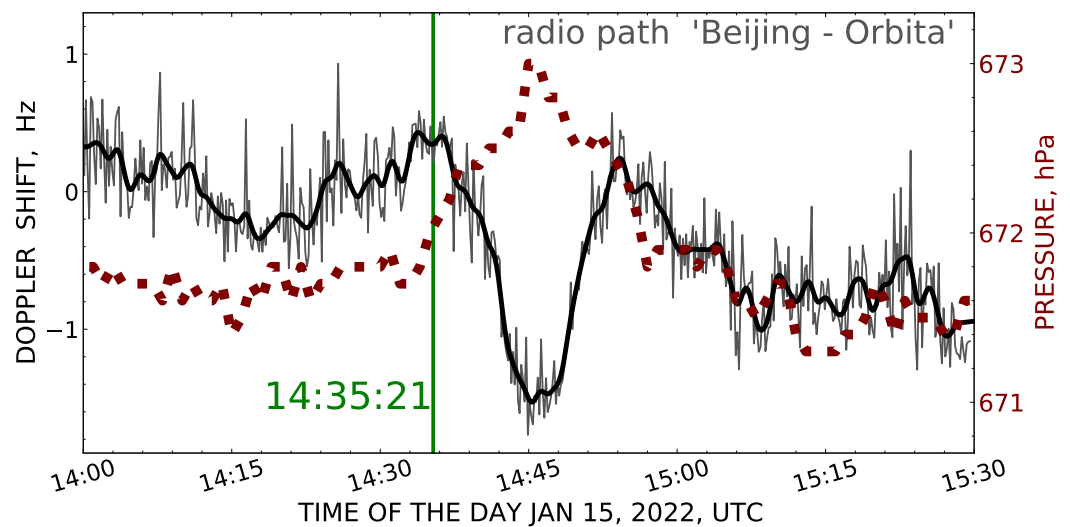
Figure 6. Comparison of the data on the Doppler frequency shift on the Beijing radio polygon "Orbita" radio path registered on 15 January 2022 and the time history of atmospheric pressure as it was measured at the Tien Shan station (dotted line). The thin solid line corresponds to the original measurement data of the Doppler signal, and the bold line corresponds to the same data after smoothing using a 10-point running average filter. The record of barometric pressure is displaced to -1.50 h along the time axis (see text).

As it follows from Figure 6, the duration of the period of anomalous Doppler frequency shift is reasonably close to that of the atmospheric pressure pulse, and the start moments of both effects practically coincide. The distribution speed of the two anomalous effects also seems to be practically identical, about 0.306 km·s^{-1}, as discussed in the above paragraphs. These experimental facts mean that both anomalies originated from the same acoustic disturbance, which arose at a height of about 100 km and propagated at the velocity of a surface Lamb wave. In turn, the specific features of these phenomena permit us to estimate the order of energy that was transferred into the atmosphere upon the considered explosion event.

Since the average energy of an air molecule is $\frac{3}{2}kT$, the energy density of the atmosphere equals $\frac{3}{2}nkT$, where n is the concentration of molecules, T is the temperature, and k is the Boltzmann constant. The barometric pressure (p) is connected with the molecule concentration by an equation of state, $p = nkT$. As a result, the energy density can be expressed through the atmospheric pressure as

$$\varepsilon = \frac{3}{2}p. \tag{1}$$

The total energy (ΔE) transmitted to the mass of atmosphere by the Hunga Tonga eruption can be found as a product of the disturbed energy density, $\Delta \varepsilon = \frac{3}{2}\Delta p$, and the effective spatial volume of the disturbance region (V_{eff}),

$$V_{eff} = 2\pi r_\oplus \sin\left(\frac{r}{r_\oplus}\right) H\tau c_s. \tag{2}$$

where $r_\oplus$ is the radius of the Earth; r is the distance to the eruption point; $2\pi r_\oplus \sin\left(\frac{r}{r_\oplus}\right)$ is the length of the circumference of the disturbance front on the Earth's spherical surface; τ and c_s are, correspondingly, the time duration of the disturbance and the sound speed; and H is the height of the homogeneous atmosphere in which the surface Lamb wave concentrates. Finally, a simple expression for the transferred energy (ΔE) is

$$\Delta E = 3\pi\Delta p r_\oplus \sin\left(\frac{r}{r_\oplus}\right) H\tau c_s. \tag{3}$$

According to the measurement data presented above, at the Tien Shan mountain station ($r = 12948 \times 10^3$ m), the average amplitude of the pulse of atmospheric pressure was $\Delta p \approx 0.65$ hPa, and the pressure disturbance lasted $\tau \approx 1000$ s and had propagation speed $c_s = 306$ m·s^{-1}. Putting these values together into Equation (3) and taking into account that 1 hPa = 100 Pa [J·m^{-3}], $r_\oplus = 6371 \times 10^3$ m, $H = 8 \times 10^3$ m, and 4.184×10^{15} J = 1 Mt$_{\text{TNT}}$, the following is the rough estimate of the energy released into the atmosphere by the Hunga Tonga explosive eruption, expressed in megatons of TNT equivalent:

$$\Delta E \approx 2 \times 10^3 \text{ Mt}_{\text{TNT}}. \tag{4}$$

4. Conclusions

The measurement equipment installed at radio polygon "Orbita" and at the Tien Shan mountain scientific station registered disturbances of the near-surface atmosphere, of the ionosphere, and of variations in telluric current that took place after the explosion of the Hunga Tonga volcano on 15 January 2022. In this experiment, the monitoring of the atmospheric pressure, of the Doppler frequency shift of the ionospheric signal, and of telluric current in the near-surface layers of the ground was made at a considerable distance, of about 12×10^3 km, from the volcano. The observations may be summarized as follows:

1. On 15 January 2022, 11 h, 46 min, and 10 s after the volcano explosion, an anomalous short-time pulse of the atmospheric pressure was detected; it had an amplitude of 1.3 hPa and duration of about (25–30) min and propagated in the atmosphere at the velocity of Lamb waves, 0.3056 km·s^{-1}, as it was registered by the barometer of the Tien Shan mountain station.

2. The continuous monitoring of the Doppler frequency shift of the ionospheric signal on the inclined radio paths with lengths of 3212 km (7245 kHz) and 2969 km (5860 kHz) permitted us to reveal two different ionosphere disturbances on the day of the Hunga Tonga explosive eruption. The disturbance onset time corresponded to the arrival of the atmospheric waves moving at velocities of 0.3059 km·s^{-1} and 0.2602 km·s^{-1} at the reflection point of radio waves in the ionosphere. Judging by the velocity values, the observed disturbances of the Doppler frequency shift of the ionospheric signal arose as a result of the successive passage of the Lamb- and acoustic-gravity waves generated by the volcano explosion and their influence on the ionosphere.

3. On the day of the volcano explosion, two consecutive disturbances of the variations in telluric current were found, with their appearance being consistent with the passage of the atmospheric waves at velocities of 0.3056 km·s^{-1} and 0.2600 km·s^{-1}. Both velocity estimates permitted us to connect the observed effects to the passage of the Lamb and acoustic-gravity waves from the volcano explosion at the point of the telluric current registration. Thus, the atmospheric waves, propagating across the whole thickness of the atmosphere, caused the modulation of the electric currents in the

ionosphere, which induced an electromagnetic response of telluric current registered at the ground level.

4. The energy transferred into the atmosphere upon the explosion of the Hunga Tonga volcano was roughly estimated using the parameters of the Lamb wave as 2000 Mt of TNT equivalent.

References

1. Kulichkov, S.N.; Chunchuzov, I.P.; Popov, O.E.; Gorchakov, G.I.; Mishenin, A.A.; Perepelkin, V.G.; Bush, G.A.; Skorokhod, A.I.; Vinogradov, Y.A.; Semutnikova, E.G.; et al. Acoustic-gravity Lamb waves from the eruption of the Hunga-Tonga–Hunga-Hapai volcano, its energy release and impact on aerosol concentrations and tsunami. *Pure Appl. Geophys.* **2022**, *179*, 1533–1548. [CrossRef]
2. Matoza, R.S.; Fee, D.; Assink, J.D.; Iezzi, A.M.; Green, D.N.; Kim, K.; Toney, L.; Lecocq, T.; Krishnamoorthy, S.; Lalande, J.-M.; et al. Atmospheric waves and global seismoacoustic observations of the January 2022 Hunga eruption, Tonga. *Science* **2022**, *377*, 95. [CrossRef] [PubMed]
3. Chen, C.-H.; Zhang, X.; Sun, Y.-Y.; Wang, F.; Liu, T.-C.; Lin, C.-Y.; Gao, Y.; Lyu, J.; Jin, X.; Zhao, X.; et al. Individual wave propagations in ionosphere and troposphere triggered by the Hunga Tonga–Hunga Ha´apai underwater volcano eruption on 15 January 2022. *Remote Sens.* **2022**, *14*, 2179. [CrossRef]
4. Kubota, T.; Saito, T.; Nishida, K. Global fast-traveling tsunamis driven by atmospheric Lamb waves on the 2022 Tonga eruption. *Science* **2022**, *377*, 91–94. [CrossRef] [PubMed]
5. Wright, C.J.; Hindley, N.P.; Alexander, M.J.; Barlow, M.; Hoffmann, L.; Mitchell, C.N.; Prata, F.; Bouillon, M.; Carstens, J.; Clerbaux, C.; et al. Surface-to-space atmospheric waves from Hunga Tonga–Hunga Ha´apai eruption. *Nature* **2022**, *609*, 741–746. [CrossRef]
6. Heki, K. Ionospheric signatures of repeated passages of atmospheric waves by the 2022 Jan. 15 Hunga Tonga–Hunga Ha´apai eruption detected by QZSS–TEC observations in Japan. *Earth Planets Space* **2022**, *74*, 112. [CrossRef]
7. Themens, D.R.; Watson, C.; Žagar, N.; Vasylkevych, S.; Elvidge, S.; McCaffrey, A.; Prikryl, P.; Reid, B.; Wood, A.; Jayachandran, P.T. Global propagation of ionospheric disturbances associated with the 2022 Tonga volcanic eruption. *Geophys. Res. Lett.* **2022**, *49*, e2022GL0981582. [CrossRef]
8. Zhang, S.-R.; Vierinen, J.; Aa, E.; Goncharenko, L.P.; Erickson, P.J.; Rideout, W.; Coster, A.J.; Spicher, A. 2022 Tonga volcanic eruption induced global propagation of ionospheric disturbances via Lamb waves. *Front. Astron. Space Sci.* **2022**, *9*, 871275. [CrossRef]
9. Aa, E.; Zhang, S.; Wang, W.; Erickson, P.J.; Qian, L.; Eastes, R.; Harding, B.J.; Immel, T.J.; Karan, D.K.; Daniell, R.E.; et al. Pronounced suppression and X-pattern merging of equatorial ionization anomalies after the 2022 Tonga volcano eruption. *J. Geophys. Res. Space Phys.* **2022**, *127*, e2022JA030527. [CrossRef]
10. Cahyadi, M.N.; Handoko, E.Y.; Rahayu, R.W.; Heki, K. Comparison of volcanic explosions in Japan using impulsive ionospheric disturbances. *Earth Planets Space* **2021**, *73*, 228. [CrossRef]
11. Heki, K.; Fujimoto, T. Atmospheric modes excited by the 2021 August eruption of the Fukutoku–Okanoba volcano, Izu–Bonin Arc, observed as harmonic TEC oscillations by QZSS. *Earth Planets Space* **2022**, *74*, 27. [CrossRef]
12. Shepetov, A.; Kryakunova, O.; Mamina, S.; Ryabov, V.; Saduyev, N.; Sadykov, T.; Salikhov, N.; Vildanova, L.; Zhukov, V. Geophysical Aspect of Cosmic Ray Studies at the Tien Shan Mountain Station: Monitoring of Radiation Background, Investigation of Atmospheric Electricity Phenomena in Thunderclouds, and the Search for the Earthquake Precursor Effects. *Phys. At. Nucl.* **2021**, *84*, 1128–1136. [CrossRef]

13. Salikhov, N.M.; Argynova, K.A.; Vildanova, L.I.; Zhukov, V.V.; Idrisova, T.K.; Iskakov, B.M.; Mamina, S.A.; Pak, G.D.; Ryabov, V.A.; Saduyev, N.O.; et al. Multichannel monitoring of the radiation background and a search for precursor signals of the seismic activity at the Tien Shan Mountain Station. *Bull. Lebedev Phys. Inst.* **2022**, *49*, 317–321. [CrossRef]

14. Salikhov, N.M.; Somsikov, V.M. The program- and hardware complex for registration of the Doppler frequency shift of ionosphere radio-signal over earthquake epicenters. *Bull. Nat. Acad. Sci. Kazakhstan Repub.* **2014**, *296*, 115–121. (In Russian)

15. Salikhov, N.M. New registration method of the dynamic of ionosphere ionization bursts by the program- and hardware complex of Doppler measurements on a slanted radio-track. *Bull. Nat. Acad. Sci. Kazakhstan Repub.* **2016**, *308*, 27–33. (In Russian)

16. Drobzhev, V.I.; Krasnov, V.M.; Salikhov, N.M. Ionospheric disturbances accompanying earthquakes and explosions. *Radiophys. Quant. Electr.* **1978**, *21*, 1295–1296. [CrossRef]

17. Drobzhev, V.I.; Zheleznyakov, E.V.; Idrisov, I.K.; Kaliev, M.Z.; Kazakov, V.V.; Krasnov, V.M.; Pelenitsyn, G.M.; Savel'Ev, V.L.; Salikov, N.M.; Shingarkin, A.D. Ionospheric effects of the acoustic wave above the epicenter of an industrial explosion. *Radiophys. Quant. Electr.* **1987**, *30*, 1047–1051. [CrossRef]

18. Laštovička, J.; Chum, J. A review of results of the international ionospheric Doppler sounder network. *Adv. Space Res.* **2017**, *60*, 1629–1643. [CrossRef]

19. Krasnov, V.M.; Drobzheva, Y.V.; Chum, J. Far-field coseismic ionospheric disturbances of Tohoku earthquake. *J. Atmos. Sol. Terr. Phys.* **2015**, *135*, 12–21. [CrossRef]

20. Salikhov, N.; Shepetov, A.; Pak, G.; Nurakynov, S.; Ryabov, V.; Saduyev, N.; Sadykov, T.; Zhantayev, Z.; Zhukov, V. Monitoring of gamma radiation prior to earthquakes in a study of lithosphere-atmosphere-ionosphere coupling in Northern Tien Shan. *Atmosphere* **2022**, *13*, 1667. [CrossRef]

21. Salikhov, N.M.; Pak, G.D. Ionospheric effects of solar flares and earthquake according to Doppler frequency shift on an inclined radio path. *Bull. Nat. Acad. Sci. Kazakhstan Repub.* **2020**, *331*, 108–115. [CrossRef]

22. The Tien-Shan Mountain Station's Database. Available online: http://www.tien-shan.org (accessed on 1 December 2022).

23. SHORT-WAVE.INFO. Available online: https://www.short-wave.info (accessed on 1 December 2022).

24. Salikhov, N.; Pak, G.; Shepetov, A.; Zhukov, V.; Seifullina, B. Hardware-Software Complex for the telluric current investigation in a seismically hazardous region of Zailiysky Alatau. *News Nat. Acad. Sci. Kazakhstan Repub. Ser. Geol. Tech. Sci.* **2021**, *5*, 94–102. [CrossRef]

25. SENSOR.COMMUNITY. Available online: https://archive.sensor.community (accessed on 1 December 2022).

26. Kanamori, H.; Mori, J.; Harkrider, D.G. Excitation of atmospheric oscillations by volcanic eruptions. *J. Geophys. Res.* **1994**, *99*, 21947–21961. [CrossRef]

27. Harding, B.J.; Wu, Y.J.; Alken, P.; Yamazaki, Y.; Triplett, C.C.; Immel, T.J.; Gasque, L.C.; Mende, S.B.; Xiong, C. Impacts of the January 2022 Tonga volcanic eruption on the ionospheric dynamo: ICON-MIGHTI and Swarm observations of extreme neutral winds and currents. *J. Geophys. Res. Lett.* **2022**, *49*, e2022GL098577. [CrossRef]

28. Drobzhev, V.I.; Krasnov, V.M.; Salikhov, N.M. Simultaneous spectral analysis of wave perturbations in the ionospheric D-layer and F-layer. *Radiophys. Quant. Electr.* **1979**, *22*, 168–169. [CrossRef]